

## A UAPO-BASED SOLUTION FOR THE SCATTERING BY A LOSSLESS DOUBLE-NEGATIVE METAMATERIAL SLAB

G. Gennarelli and G. Riccio

Dipartimento di Ingegneria dell' Informazione ed Ingegneria Elettrica  
Università di Salerno  
via Ponte Don Melillo, Fisciano (SA) I-84084, Italy

**Abstract**—A closed form solution is here proposed for evaluating the field diffracted by the edge of a lossless, isotropic and homogeneous double-negative metamaterial slab when illuminated by a plane wave at skew incidence. It is obtained by considering a Physical Optics approximation of the electric and magnetic equivalent surface currents in the radiation integral and by performing a uniform asymptotic evaluation of this last. The final expression is given in terms of the Geometrical Optics response of the structure and the standard transition function of the Uniform Geometrical Theory of Diffraction, so that it results easy to handle and simple to implement in a computer code. As demonstrated by numerical tests, it allows one to compensate the discontinuities of the Geometrical Optics field at the reflection and incidence shadow boundaries. Moreover, the accuracy of the solution is well assessed by means of comparisons with a commercial tool based on Finite Element Method.

### 1. INTRODUCTION

In recent years, double-negative (DNG) metamaterials (MTMs) have attracted considerable attention because of their interesting properties and applications in microwave and optical devices [1–3]. DNG MTMs have negative permittivity and permeability simultaneously, so that they are characterized by antiparallel phase and group velocities, or negative refractive index. Accordingly, an electromagnetic (EM) wave incident upon the interface between a conventional double-positive (DPS) material and a DNG MTM undergoes negative refraction, corresponding to a negative refraction angle. This suggests that the

---

Corresponding author: G. Riccio (riccio@diie.unisa.it).

refraction is anomalous, and the refraction angle is on the same side of the incident one. DNG MTMs can be artificially fabricated by embedding various classes of small inclusions in host media (volumetric DNG MTMs) or by connecting inhomogeneities to host surfaces (planar DNG MTMs), and may be engineered to have new physically realizable response functions that do not occur, or may not be readily available, in nature.

The target of the present work is an efficient solution for evaluating the field scattered by a truncated lossless DNG MTM slab when illuminated by a plane wave at skew incidence (see Fig. 1). The study is simplified by assuming that the medium under discussion is isotropic and homogeneous.

It must be stressed that, because of the finite nature of practical structures and devices, the important effects arising from wave diffraction at edges of DNG MTM slabs cannot be ignored. As a matter of fact, DNG MTM planar slabs of only infinite extent have been considered in most previous theoretical studies. Numerical methods can be used to solve EM scattering problems involving MTMs (see [4–9] as reference), but they become very poorly convergent, inefficient, and sometimes even intractable when considering structures large in terms of the EM wavelength. Moreover, the propagation mechanisms are not easy to understand from the physical point of view if the conventional numerical methods are adopted. The Geometrical Theory of Diffraction (GTD) represents a very interesting alternative approach for solving high frequencies problems concerning electrically large MTM scatterers. It provides a very powerful and physically appealing simple ray theory for describing and quantifying the wave diffraction mechanism at the edge of a truncated structure, and allows one to calculate the total field at an observation point in the surrounding space in terms of direct, reflected/transmitted and diffracted ray fields. In this framework, a Uniform Geometrical Theory of Diffraction (UTD) for predicting the radiation by sources near thin planar DPS/DNG material discontinuities has been recently proposed in [10]. It has been obtained via a partially heuristic spectral synthesis approach and recovers the proper local plane wave Fresnel's reflection and transmission coefficients and surface wave constants of the DPS/DNG material. With reference to the here tackled problem, the analytical difficulties are attenuated by considering a truncated DNG MTM planar slab as a canonical penetrable half-plane. The derivation of the exact solution for the diffracted field is a hard task, and an approximate "practical" solution, which is efficient and simple to handle, becomes very appealing from the engineering point of view.

The first step of the proposed approach concerns the evaluation

of the reflection and transmission coefficients, i.e., the Geometrical Optics (GO) response of the considered penetrable structure. They are obtained by following the approach reported in [11], which is based on the results derived by Kong in [12], and contain the geometric, electric and magnetic characteristics of the DNG MTM planar slab. In the second step, electric and magnetic Physical Optics (PO) surface currents are assumed as equivalent sources of the scattered field, and expressed in terms of the reflection and transmission coefficients. At last, a useful approximation and a uniform asymptotic evaluation of the resulting radiation integral allow one to formulate the diffracted ray field in terms of the GO response and the UTD transition function [13]. The here derived expression belongs to the set of the Uniform Asymptotic PO (UAPO) solutions developed in recent years to solve many diffraction problems (see [14] as reference). Some comparisons with COMSOL MULTIPHYSICS<sup>®</sup> simulations are reported in order to assess the accuracy of the here proposed UAPO-based method for the evaluation of the field scattered by a truncated DNG MTM planar slab.

## 2. THE GO RAY FIELD

A linearly polarized plane wave impinging on a lossless DNG MTM planar slab of infinite extent, surrounded by free space, is considered in the following. The layer thickness is  $d$  and its relative electric permittivity and relative magnetic permeability are  $\epsilon_r = -|C|$  and  $\mu_r = -1$ , respectively.

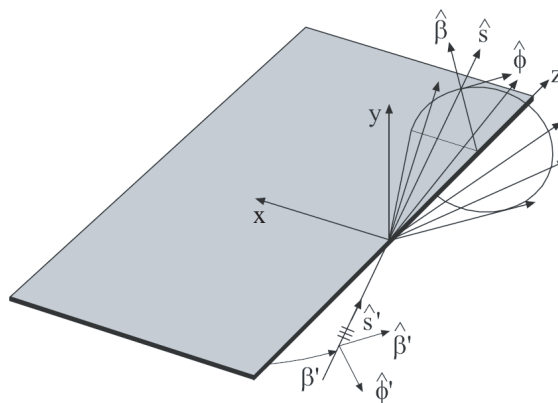


**Figure 1.** Diffraction by a lossless DNG MTM slab.

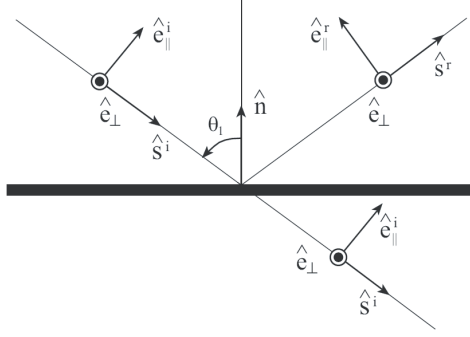


**Figure 2.** Ray-fixed coordinate systems in the incidence plane.

In order to determine the GO response in the ordinary plane of incidence, it is convenient to consider the local ray-fixed reference systems shown in Fig. 2. The face illuminated by the incident plane wave is here assumed as reference face for the evaluation of the reflection and transmission coefficients. Accordingly, it results:

$$\begin{pmatrix} E_{\parallel}^r \\ E_{\perp}^r \end{pmatrix} = \underline{\underline{R}} \begin{pmatrix} E_{\parallel}^i \\ E_{\perp}^i \end{pmatrix} = \begin{pmatrix} R_{\parallel} & 0 \\ 0 & R_{\perp} \end{pmatrix} \begin{pmatrix} E_{\parallel}^i \\ E_{\perp}^i \end{pmatrix} \quad (1)$$

$$\begin{pmatrix} E_{\parallel}^t \\ E_{\perp}^t \end{pmatrix} = \underline{\underline{T}} \begin{pmatrix} E_{\parallel}^i \\ E_{\perp}^i \end{pmatrix} = \begin{pmatrix} T_{\parallel} & 0 \\ 0 & T_{\perp} \end{pmatrix} \begin{pmatrix} E_{\parallel}^i \\ E_{\perp}^i \end{pmatrix} \quad (2)$$

wherein  $\parallel$  and  $\perp$  denote the incident, reflected and transmitted field components parallel and perpendicular to the ordinary plane of incidence. Note that in the case of an EM wave impinging on a DPS/DNG interface, negative refraction arises, and this corresponds to a refraction angle on the same side of the incident one. The elements of the reflection  $\underline{\underline{R}}$  and transmission  $\underline{\underline{T}}$  matrices are determined by taking into account this anomalous refraction and by following the approach reported in [11], which is based on the results derived by Kong in [12]. They contain the geometric, electric and magnetic characteristics of the DNG MTM planar slab and can be so expressed:

$$R_{\parallel, \perp} = \frac{\overline{R}_{12_{\parallel, \perp}} + \overline{R}_{23_{\parallel, \perp}} e^{j2\gamma}}{1 + \overline{R}_{12_{\parallel, \perp}} \overline{R}_{23_{\parallel, \perp}} e^{j2\gamma}} \quad (3)$$

$$\overline{R}_{ij_{\parallel}} = \frac{k_j \cos \vartheta_i - k_i \cos \vartheta_j}{k_j \cos \vartheta_i + k_i \cos \vartheta_j} \quad (4)$$

$$\overline{R}_{ij_{\perp}} = \frac{k_i \cos \vartheta_i - k_j \cos \vartheta_j}{k_i \cos \vartheta_i + k_j \cos \vartheta_j} \quad (5)$$

$$T_{\parallel,\perp} = \frac{\bar{T}_{12,\perp} \bar{T}_{23,\perp} e^{j\gamma}}{1 + \bar{R}_{12,\perp} \bar{R}_{23,\perp} e^{j2\gamma}} \tag{6}$$

$$\bar{T}_{ij\parallel} = \frac{2k_i \cos \vartheta_i}{k_j \cos \vartheta_i + k_i \cos \vartheta_j} \tag{7}$$

$$\bar{T}_{ij\perp} = \frac{2k_i \cos \vartheta_i}{k_i \cos \vartheta_i + k_j \cos \vartheta_j} \tag{8}$$

in which  $k_2$  is the DNG MTM wave-number,  $k_1 = k_3 = k_0$ , where  $k_0$  is the free space wave-number,  $\gamma = k_2 d \cos \vartheta_2$ , where  $\vartheta_2$  is the negative refraction angle, and the subscripts  $i$  and  $j$  refer to the left and right media involved in the propagation mechanism as shown in Fig. 3.

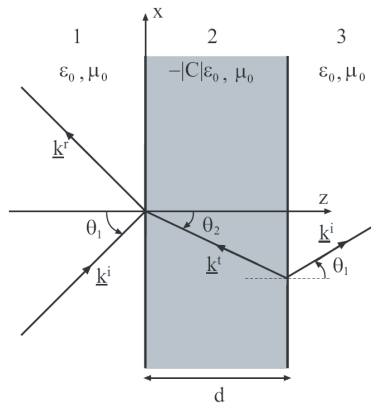


**Figure 3.** Ray transmission through a DNG MTM slab.

### 3. A UAPO SOLUTION FOR THE DIFFRACTED RAY FIELD

The analytical difficulties encountered when considering the edge contribution in truncated structures are often attenuated by modelling them as half-planes. This model is also adopted for a truncated DNG MTM planar slab from this point on, and the corresponding GO response is given according to the formulation reported in the previous Section.

The geometry of a half-plane illuminated by an arbitrary incident plane wave is sketched in Fig. 1. The  $z$ -axis of a reference coordinate system is directed along the edge and the  $x$ -axis is on the illuminated face. The angles  $(\beta', \phi')$  fix the incidence direction; the first is a measure of the skewness with respect to the edge ( $\beta' = \pi/2$  corresponds

to the normal incidence) and the latter gives the aperture of the edge-fixed plane of incidence with respect to the illuminated face ( $\phi' = 0$  corresponds to the grazing incidence). The observation direction is specified by  $(\beta, \phi)$  in a similar way.

As well-known, in the far-field approximation, the electric field generated by electric and magnetic PO surface currents  $\underline{J}_s^{PO}$  and  $\underline{J}_{ms}^{PO}$  surrounded by free space can be expressed by means of the following radiation integral:

$$\underline{E}^s \cong -jk_0 \iint_S \left[ \left( \underline{I} - \hat{R}\hat{R} \right) (\zeta_0 \underline{J}_s^{PO}) + \underline{J}_{ms}^{PO} \times \hat{R} \right] \frac{e^{-jk_0|r-r'|}}{4\pi|r-r'|} dS \quad (9)$$

wherein  $\zeta_0$  is the free space impedance,  $\underline{r}$  and  $\underline{r}'$  denote the observation and source points, respectively,  $\hat{R}$  is the unit vector from the radiating element at  $\underline{r}'$  to the observation point, and  $\underline{I}$  is the  $(3 \times 3)$  identity matrix. In the here proposed approach, the involved currents represent equivalent sources originated by the discontinuities of the tangential components of the magnetic and electric fields across the slab, and can be so expressed:

$$\zeta_0 \underline{J}_s^{PO} = \zeta_0 \tilde{\underline{J}}_s^{PO} e^{jk_0(x' \sin \beta' \cos \phi' - z' \cos \beta')} \quad (10)$$

$$\underline{J}_{ms}^{PO} = \tilde{\underline{J}}_{ms}^{PO} e^{jk_0(x' \sin \beta' \cos \phi' - z' \cos \beta')} \quad (11)$$

where  $(x', z')$  denotes the integration point on the half-plane, and

$$\zeta_0 \tilde{\underline{J}}_s^{PO} = [1 - R_\perp - T_\perp] E_\perp^i \cos \vartheta_1 \hat{e}_\perp + [1 + R_\parallel - T_\parallel] E_\parallel^i \hat{t} \quad (12)$$

$$\tilde{\underline{J}}_{ms}^{PO} = [1 - R_\parallel - T_\parallel] E_\parallel^i \cos \vartheta_1 \hat{e}_\perp - [1 + R_\perp - T_\perp] E_\perp^i \hat{t} \quad (13)$$

with  $\hat{t} = \hat{n} \times \hat{e}_\perp = \hat{y} \times \hat{e}_\perp$ . The incident field components relevant to the ordinary plane of incidence can be simply related to those in the incident ray-fixed reference system  $(\hat{s}', \hat{\beta}', \hat{\phi}')$ , i.e.,

$$\begin{aligned} \begin{pmatrix} E_\parallel^i \\ E_\perp^i \end{pmatrix} &= \underline{M}_1 \begin{pmatrix} E_{\beta'}^i \\ E_{\phi'}^i \end{pmatrix} \\ &= \frac{1}{\sqrt{1 - \sin^2 \beta' \sin^2 \phi'}} \begin{pmatrix} \cos \beta' \sin \phi' & \cos \phi' \\ -\cos \phi' & \cos \beta' \sin \phi' \end{pmatrix} \begin{pmatrix} E_{\beta'}^i \\ E_{\phi'}^i \end{pmatrix} \end{aligned} \quad (14)$$

where  $E_{\beta'}^i$  and  $E_{\phi'}^i$  are the field components (at the origin) along  $\hat{\beta}' = \hat{\phi}' \times \hat{s}'$  and  $\hat{\phi}' = (\hat{s}' \times \hat{z})/|\hat{s}' \times \hat{z}|$ , respectively,  $\hat{s}' = (-\sin \beta' \cos \phi', -\sin \beta' \sin \phi', \cos \beta')$  being the unit vector of the incidence direction (see Fig. 1).

Since the diffraction is confined to the Keller's cone ( $\beta = \beta'$ ), if  $\hat{s} = (\sin \beta' \cos \phi, \sin \beta' \sin \phi, \cos \beta')$  is the unit vector of the diffraction direction, the approximation  $\hat{R} = \hat{s}$  is permitted for evaluating the edge diffracted field [15]. Accordingly, at the observation point  $P(x, y, z)$  it results:

$$\underline{E}^s \cong \left[ (\underline{I} - \hat{s}\hat{s}) \left( \zeta_0 \underline{\tilde{J}}_s^{PO} \right) + \underline{\tilde{J}}_{ms}^{PO} \times \hat{s} \right] I_0 \tag{15}$$

with

$$I_0 = -jk_0 \int_0^{+\infty} e^{jk_0 x' \sin \beta' \cos \phi'} \int_{-\infty}^{+\infty} e^{-jk_0 z' \cos \beta'} \frac{e^{-jk_0 \sqrt{(x-x')^2 + y^2 + (z-z')^2}}}{4\pi \sqrt{(x-x')^2 + y^2 + (z-z')^2}} dz' dx' \tag{16}$$

Analytical manipulations and integrations lead to:

$$I_0 = \frac{e^{-jk_0 z \cos \beta'}}{2(2\pi j) \sin \beta'} \int_C \frac{e^{-jk_0 \rho \sin \beta' \cos(\alpha \mp \phi)}}{\cos \alpha + \cos \phi'} d\alpha \tag{17}$$

where  $\rho = \sqrt{x^2 + y^2}$  is the radial distance,  $C$  is the integration path in the complex  $\alpha$ -plane (see Fig. 4), and  $-$  ( $+$ ) sign applies if  $0 < \phi < \pi$  ( $\pi < \phi < 2\pi$ ). By applying the Cauchy's theorem, the contribution to the field related to the integration along  $C$  (distorted for the presence of singularities in the integrand) is equivalent to the summation of the integral along the Steepest Descent Path ( $SDP$ ), passing through the pertinent saddle-point, and the residue contributions associated with all those poles that are inside the closed path  $C + SDP$ . The UAPO edge diffraction contribution  $\underline{E}^d$  can be obtained by performing a uniform

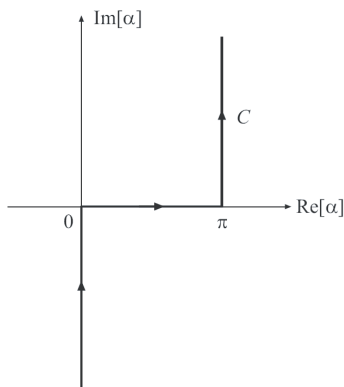


Figure 4. Integration path  $C$ .

asymptotic evaluation of the integral along the *SDP*. Accordingly, in the diffracted ray-fixed reference system it results:

$$\begin{aligned} \underline{E}^d &= \begin{pmatrix} E_\beta^d \\ E_\phi^d \end{pmatrix} = \underline{\underline{D}} \begin{pmatrix} E_{\beta'}^i \\ E_{\phi'}^i \end{pmatrix} \frac{e^{-jk_0s}}{\sqrt{s}} \\ &= \frac{e^{-j\pi/4}}{2\sqrt{2\pi k_0} \sin^2 \beta'} \frac{F_t(2k_0s \sin^2 \beta' \cos^2(\phi \pm \phi')/2)}{\cos \phi + \cos \phi'} \underline{\underline{M}} \begin{pmatrix} E_{\beta'}^i \\ E_{\phi'}^i \end{pmatrix} \frac{e^{-jk_0s}}{\sqrt{s}} \end{aligned} \quad (18)$$

where  $s$  is the distance along the diffracted ray and  $F_t(\cdot)$  is the UTD transition function [13]. The matrix  $\underline{\underline{M}}$  is given in Appendix and accounts for the GO response of the DNG MTM half-plane and for proper coordinate transformations.

#### 4. NUMERICAL RESULTS

The effectiveness of the proposed solution has been assessed by means of numerical tests. The DNG MTM slab considered in the here reported results is characterized by  $\varepsilon_r = -4$  and  $d = 0.125 \lambda_0$ ,  $\lambda_0$  being the free-space wavelength. The first set of figures ranging from Fig. 5 to Fig. 8 refers to an incident plane wave propagating in the direction  $\beta' = 60^\circ$ ,  $\phi' = 20^\circ$  and having the electric field linearly polarized along  $\hat{\beta}'$  ( $E_{\beta'}^i = 1$ ,  $E_{\phi'}^i = 0$ ). The field is evaluated over a circular path

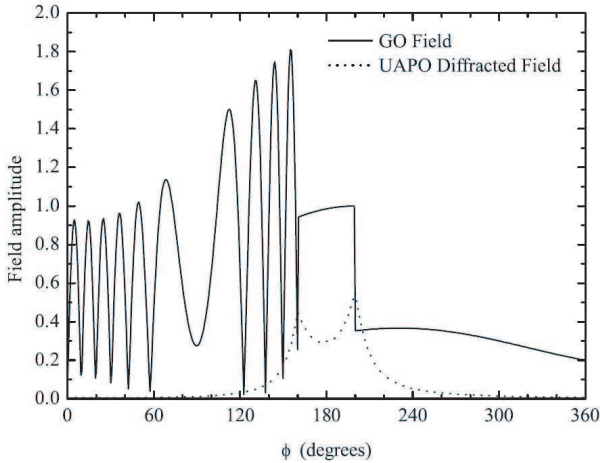


**Figure 5.** Amplitude of the electric field  $\beta$ -component related to the GO and UAPO contributions. Incident field:  $E_{\beta'}^i = 1$ ,  $E_{\phi'}^i = 0$ . Incidence direction:  $\beta' = 60^\circ$ ,  $\phi' = 20^\circ$ . Observation path:  $\rho = 10\lambda_0$ .

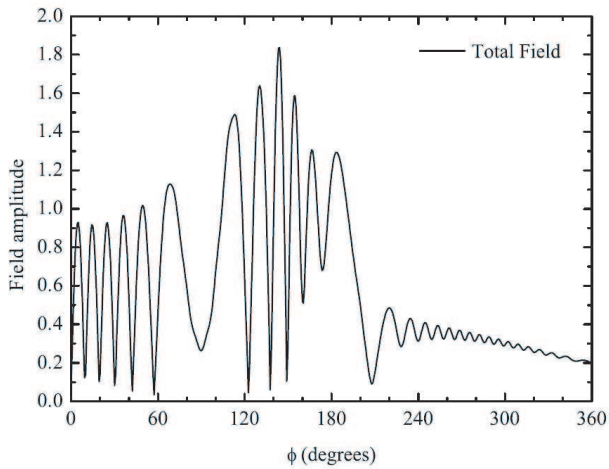


**Figure 6.** Amplitude of the electric field  $\beta$ -component related to the total field. Incident field:  $E_{\beta'}^i = 1$ ,  $E_{\phi'}^i = 0$ . Incidence direction:  $\beta' = 60^\circ$ ,  $\phi' = 20^\circ$ . Observation path:  $\rho = 10\lambda_0$ .

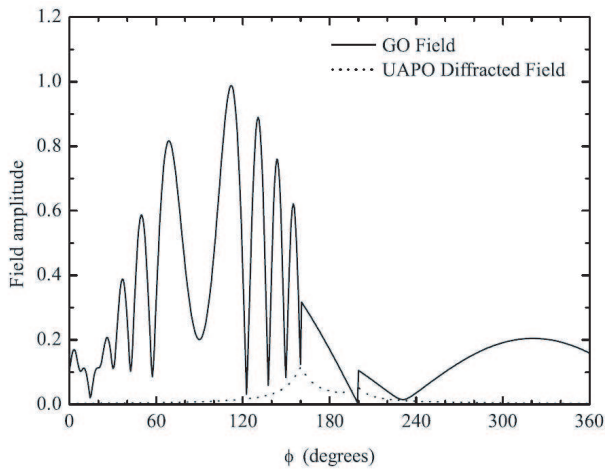


**Figure 7.** Amplitude of the electric field  $\phi$ -component related to the GO and UAPO contributions. Incident field:  $E_{\beta'}^i = 1$ ,  $E_{\phi'}^i = 0$ . Incidence direction:  $\beta' = 60^\circ$ ,  $\phi' = 20^\circ$ . Observation path:  $\rho = 10\lambda_0$ .

with radius  $\rho = 10\lambda_0$ . The magnitudes of the  $\beta$ -components of the GO and UAPO diffracted ray fields are reported versus  $\phi$  in Fig. 5. As expected, the GO field has two discontinuities in correspondence of the reflection and incidence/transmission shadow boundaries at  $\phi = 160^\circ$

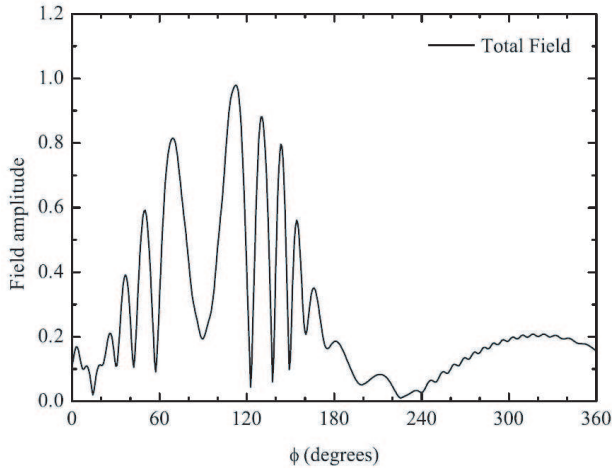


**Figure 8.** Amplitude of the electric field  $\phi$ -component related to the total field. Incident field:  $E_{\beta'}^i = 1$ ,  $E_{\phi'}^i = 0$ . Incidence direction:  $\beta' = 60^\circ$ ,  $\phi' = 20^\circ$ . Observation path:  $\rho = 10\lambda_0$ .

and  $\phi = 200^\circ$ . On the other hand, the UAPO diffracted field is not negligible in the neighbourhood of such boundaries and assures the continuity of the total field as confirmed by the curve shown in Fig. 6. Analogous considerations apply to the  $\phi$ -components of the GO and UAPO fields and of the total field reported in Figs. 7 and 8, respectively. Accordingly, it is possible to claim that the here derived UAPO solution for the field diffracted by the edge of a DNG MTM slab is able to perfectly compensate the GO discontinuities at the reflection and incidence/transmission shadow boundaries.

The last two figures are useful to assess the accuracy of the UAPO-based approach by means of comparisons with the UTD [10] and COMSOL MULTIPHYSICS<sup>®</sup> results in the case of normal incidence ( $\beta' = 90^\circ$ ). COMSOL MULTIPHYSICS<sup>®</sup> is a powerful interactive environment for modeling and solving problems based on partial differential equations by means of the proven Finite Element Method (FEM). The used RF module extends the COMSOL MULTIPHYSICS<sup>®</sup> modeling environment with customized user interfaces and functionality optimized for the analysis of the electromagnetic waves propagation. A  $\text{TM}_z$  polarized plane wave is considered as case study. Figs. 9 and 10 concern two incidence directions, i.e.,  $\phi' = 60^\circ$  (Fig. 9) and  $\phi' = 110^\circ$  (Fig. 10). The total field is evaluated over a circular path having  $\rho = 5\lambda_0$ . As

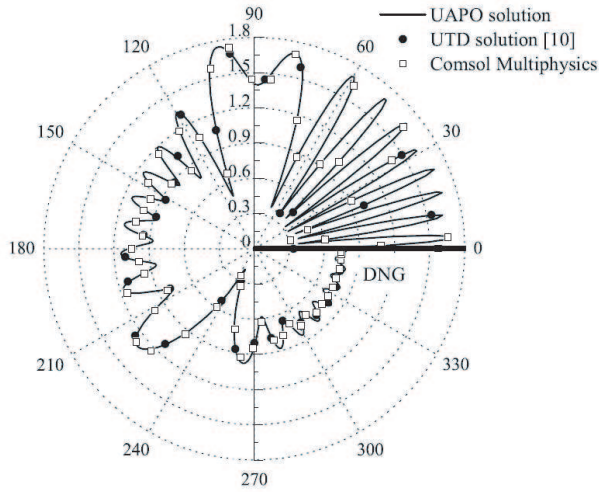


**Figure 9.** Amplitude of the total electric field  $z$ -component. Incident field:  $E_z^i = 1$ ,  $E_{\phi'}^i = 0$ . Incidence direction:  $\beta' = 90^\circ$ ,  $\phi' = 60^\circ$ . Observation path:  $\rho = 5\lambda_0$ .

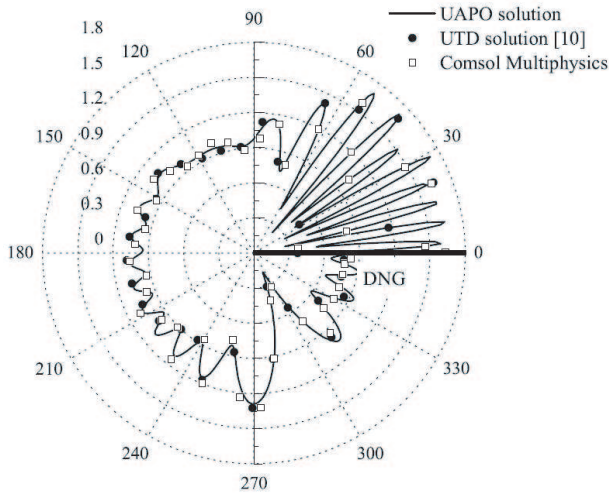


**Figure 10.** Amplitude of the total electric field  $z$ -component. Incident field:  $E_z^i = 1$ ,  $E_{\phi'}^i = 0$ . Incidence direction:  $\beta' = 90^\circ$ ,  $\phi' = 110^\circ$ . Observation path:  $\rho = 5\lambda_0$ .

can be observed, an excellent agreement with both the UTD [10] and COMSOL MULTIPHYSICS<sup>®</sup> results is attained, thus confirming the effectiveness of the here proposed solution.

## 5. CONCLUSION

A UAPO-based solution for evaluating the field scattered by a truncated DNG MTM slab illuminated by a plane wave at oblique incidence has been proposed. As a first step, the GO response of the structure has been obtained. Then, this last has been used to determine the equivalent electric and magnetic PO currents in the radiation integral. A useful approximation and a uniform asymptotic evaluation of the resulting integral have permitted to determine the UAPO diffraction coefficients. They are given in terms of the standard UTD transition function and the GO response. As shown by numerical simulations, the proposed solution exactly compensates the GO field discontinuities at the reflection and incidence/transmission shadow boundaries. Furthermore, its accuracy has been demonstrated by the very good agreement attained in the comparisons with the COMSOL MULTIPHYSICS<sup>®</sup> results. Accordingly, the UAPO-based solution is an approximate “practical” high frequency solution very appealing from the engineering point of view since it gives reliable and accurate results, is computationally efficient and easy to handle. At last, it can be surely useful in all the applications wherein truncation effects in DNG MTMs are not negligible.

## APPENDIX A.

The expression of the matrix  $\underline{\underline{M}}$  appearing in the UAPO solution (18) for the diffracted field is now made explicit. Such a matrix takes into account some useful coordinate system transformations and the expressions of  $\tilde{\underline{\underline{J}}}_s^{PO}$  and  $\tilde{\underline{\underline{J}}}_{ms}^{PO}$ , i.e.,

$$\underline{\underline{M}} = \underline{\underline{M}}_7 \left[ \underline{\underline{M}}_2 \underline{\underline{M}}_4 \underline{\underline{M}}_5 + \underline{\underline{M}}_3 \underline{\underline{M}}_4 \underline{\underline{M}}_6 \right] \underline{\underline{M}}_1 \quad (\text{A1})$$

where

$$\underline{\underline{M}}_7 = \begin{pmatrix} \cos \beta' \cos \phi & \cos \beta' \sin \phi & -\sin \beta' \\ -\sin \phi & \cos \phi & 0 \end{pmatrix} \quad (\text{A2})$$

is the transformation matrix for the edge to ray-fixed coordinate system components,

$$\underline{\underline{M}}_4 = \frac{1}{\sqrt{1 - \sin^2 \beta' \sin^2 \phi'}} \begin{pmatrix} -\cos \beta' & -\sin \beta' \cos \phi' \\ -\sin \beta' \cos \phi' & \cos \beta' \end{pmatrix} \quad (\text{A3})$$

is the transformation matrix relating the base  $\hat{e}_\perp, \hat{t}$  to  $\hat{x}, \hat{z}$ , and

$$\underline{\underline{M}}_2 = \begin{pmatrix} 1 - \sin^2 \beta' \cos^2 \phi & -\cos \beta' \sin \beta' \cos \phi \\ -\sin^2 \beta' \sin \phi \cos \phi & -\cos \beta' \sin \beta' \sin \phi \\ -\cos \beta' \sin \beta' \cos \phi & \sin^2 \beta' \end{pmatrix} \quad (\text{A4})$$

$$\underline{\underline{M}}_3 = \begin{pmatrix} 0 & -\sin \beta' \sin \phi \\ -\cos \beta' & \sin \beta' \cos \phi \\ \sin \beta' \sin \phi & 0 \end{pmatrix} \quad (\text{A5})$$

$$\underline{\underline{M}}_5 = \begin{pmatrix} 0 & [1 - R_\perp - T_\perp] \cos \vartheta_1 \\ 1 + R_\parallel - T_\parallel & 0 \end{pmatrix} \quad (\text{A6})$$

$$\underline{\underline{M}}_6 = \begin{pmatrix} [1 - R_\parallel - T_\parallel] \cos \vartheta_1 & 0 \\ 0 & -[1 + R_\perp - T_\perp] \end{pmatrix} \quad (\text{A7})$$

Note that the matrices  $\underline{\underline{M}}_5$  and  $\underline{\underline{M}}_6$  originate from the expressions of the PO surface currents, so that they contain the reflection and transmission coefficients of the considered DNG MTM slab.

## REFERENCES

1. Engheta, N. and R. W. Ziolkowski, "A positive future for double-negative metamaterials," *IEEE Trans. Microw. Theory Tech.*, Vol. 53, No. 4, 1535–1556, 2005.
2. Engheta, N. and R. W. Ziolkowski, *Metamaterials: Physics and Engineering Explorations*, Wiley-InterScience, 2006.
3. Caloz, C. and T. Itoh, *Electromagnetic Metamaterials: Transmission Line Theory and Microwave Applications*, Wiley-InterScience, Hoboken, 2006.
4. Ziolkowski, R. W. and E. Heyman, "Wave propagation in media having negative permittivity and permeability," *Phys. Rev. E*, Vol. 64, 056625:1–15, 2001.
5. Caloz, C., C. C. Chang, and T. Itoh, "Full-wave verification of the fundamental properties of left-handed materials (LHMs) in waveguide configurations," *J. App. Phys.*, Vol. 90, No. 11, 5483–5486, Dec. 2001.
6. Moss, C. D., T. M. Grzegorzczuk, Y. Zhang, and J. A. Kong, "Numerical studies of left handed metamaterials," *Progress In Electromagnetics Research*, PIER 35, 315–334, 2002.
7. Ziolkowski, R. W., "Pulsed and CW Gaussian beam interactions

- with double negative metamaterial slabs,” *Optics Express*, Vol. 11, No. 7, 662–681, Apr. 2003.
8. So, P. P. M., H. Du, and W. J. R. Hofer, “Modeling of metamaterials with negative refractive index using 2D-shunt and 3D-SCN TLM networks,” *IEEE Trans. Microwave Theory Tech.*, Vol. 53, No. 4, 1496–1505, 2005.
  9. Shi, Y. and C.-H. Liang, “Analysis of the double-negative materials using multi-domain pseudospectral time-domain algorithm,” *Progress In Electromagnetics Research*, PIER 51, 153–165, 2005.
  10. Lertwiriyaprapa, T., P. H. Pathak, and J. L. Volakis, “A UTD for predicting fields of sources near or on thin planar positive/negative material discontinuities,” *Radio Science*, Vol. 42, RS6S18, 2007.
  11. Cory, H. and C. Zach, “Wave propagation in metamaterial multi-layered structures,” *Microwave Opt. Technol. Lett.*, Vol. 40, No. 6, 460–465, 2004.
  12. Kong, J. A., “Electromagnetic wave interaction with stratified negative isotropic media,” *Progress In Electromagnetics Research*, PIER 35, 1–52, 2002.
  13. Kouyoumjian, R. G. and P. H. Pathak, “A uniform geometrical theory of diffraction for an edge in a perfectly conducting surface,” *Proc. IEEE*, Vol. 62, No. 11, 1448–1461, 1974.
  14. Gennarelli, C., G. Pelosi, C. Pochini, and G. Riccio, “Uniform asymptotic PO diffraction coefficients for an anisotropic impedance half-plane,” *Journal of Electromagnetic Waves and Applications*, Vol. 13, No. 7, 963–980, 1999.
  15. Senior, T. B. A. and J. L. Volakis, *Approximate Boundary Conditions in Electromagnetic*, IEE *Electromagnetic Waves Series*, Institution of Engineering and Technology, London, 1995.